



Symmetry and nonstoichiometry as possible origins of ferromagnetism in nanoscale oxides

Uchino, Takashi
Yoko, Toshinobu

(Citation)

Physical Review B, 85(1):012407-012407

(Issue Date)

2012-01-25

(Resource Type)

journal article

(Version)

Version of Record

(URL)

<https://hdl.handle.net/20.500.14094/90001637>



Symmetry and nonstoichiometry as possible origins of ferromagnetism in nanoscale oxides

Takashi Uchino*

Department of Chemistry, Graduate School of Science, Kobe University, Nada, Kobe 657-8501, Japan

Toshinobu Yoko

Institute for Chemical Research, Kyoto University, Uji, Kyoto 611-0011, Japan

(Received 1 November 2011; revised manuscript received 20 December 2011; published 25 January 2012)

We show through density functional theory calculations that extended magnetic states can inherently occur in oxides as the size of the crystals is reduced down to the nanometer scale. In nanoscale systems, some crystallographically perfect MgO crystallites paradoxically result in nonstoichiometric compositions, either cation deficient or oxygen deficient, owing to the finite number of constituting atoms. In structurally perfect but Mg-deficient substoichiometric nanocrystallites, the spin-triplet state is found to be more stable than the spin-singlet state, giving rise to an extended spin distribution that expands over the entire crystal. The further introduction of an Mg vacancy enables a higher spin-quintuplet state, enhancing the degree of spin polarization. According to this picture, long-range magnetic order arises from the combined effect of crystal symmetry and nonstoichiometry that can coexist exclusively in nanoscale systems. The idea can also give reasonable explanations for the unprecedented ferromagnetic features observed commonly in nanoscale oxides, including ubiquity, anisotropy, and diluteness.

DOI: [10.1103/PhysRevB.85.012407](https://doi.org/10.1103/PhysRevB.85.012407)

PACS number(s): 75.30.-m, 73.22.-f, 75.50.Dd

Magnetism in solids was thought to be well understood in terms of localized magnetic moments m and a Heisenberg exchange integral J . In oxides, the principal interaction stems from superexchange, in which the effective exchange coupling of magnetic atoms occurs via an intervening nonmagnetic oxygen atom. However, this m - J paradigm has recently been challenged by the finding of dilute magnetic semiconductors in which a few percent of the nonmagnetic cations are replaced by $3d$ transition-metal ions.¹⁻³ Subsequent investigations have further revealed that ferromagnetism can be found in closed-shell oxides doped with nonmagnetic elements or even in nondoped oxides.⁴⁻⁷ It should also be worth mentioning that ferromagnetism is found in a wide range of oxides, including MgO (Ref. 8), Al₂O₃ (Ref. 6), ZnO (Ref. 6) HfO₂ (Refs. 4 and 5), and TiO₂ (Ref. 5), with different crystallographic structures and compositions. However, there is one common tendency among the materials exhibiting this intriguing ferromagnetism; that is, they are mostly in the form of thin films or nanoparticles.⁷ This suggests that in nanoscale systems there exists an unrevealed underlying mechanism for ferromagnetism that is different from the conventional m - J paradigm.²

What is unusual about the nanoscale system? One immediate possibility would be a mechanism related to defects.^{9,10} It is indeed true that some intrinsic defects, e.g. cation and oxygen vacancies, provide paramagnetic ($S = 1/2$) states or spin-triplet ($S = 1$) states. However, these defect-related spin states are generally highly localized around the respective defects, hence requiring a sufficiently high concentration to allow possible ferromagnetic order via magnetic percolation. At present, there have been no credible mechanisms that can account for observed long-range ferromagnetic interactions in terms of localized defect states.^{2,7,11}

The other possibility, which, however, has not so far been seriously discussed and considered, is the effect of the finite number of atoms in nanocrystals. Consider an oxide with a

composition of M_xO_y . This oxide requires nx atoms for M (where n is an integer) and ny atoms for O to satisfy the stoichiometry. It should be noted, however, that this condition will not always be satisfied in the case of nanocrystals since the total number of constituent atoms is finite; it becomes odd or even depending on the size. As for the cubic MgO crystal, for example, crystallites consisting of an $N \times N \times N$ -atom block become stoichiometric when N is even; however, an odd number of N leads to, rigorously speaking, nonstoichiometry. In the latter case, the number of magnesium atoms is always larger (or smaller) than that of oxygen atoms by 1. The induced stoichiometric variation thus is very small and is virtually negligible in the case of the bulk where the number of atoms can be regarded as infinite. However, this might not be the case for nanocrystals made up of atoms on the order of a few hundred to a few thousand. Only one atom difference between metal and oxygen atoms could induce a noticeable nonstoichiometric effect on the resulting electronic structure.

To explore a possible nanometer-sized nonstoichiometric effect, we carry out density functional theory (DFT) calculations using clusters of atoms modeling cubic MgO nanocrystallites with different compositions. Previously, a number of theoretical calculations on MgO nanoclusters have been performed¹²⁻¹⁵ since MgO is often considered as a prototype of ionic oxides. It has been demonstrated that the cubic rock-salt model can be applied to MgO nanoclusters when going beyond the size range of ~ 50 atoms.¹⁵ However, most MgO clusters investigated previously are stoichiometric ones with an even number of atoms,¹²⁻¹⁵ and to our knowledge, the electronic structure of the cubic nonstoichiometric clusters, i.e. cubic clusters consisting of an odd number of atoms, has not been carefully examined.

All the DFT calculations in this Brief Report were carried out using the gradient-corrected Becke's three parameters hybrid exchange functional¹⁶ in combination with the

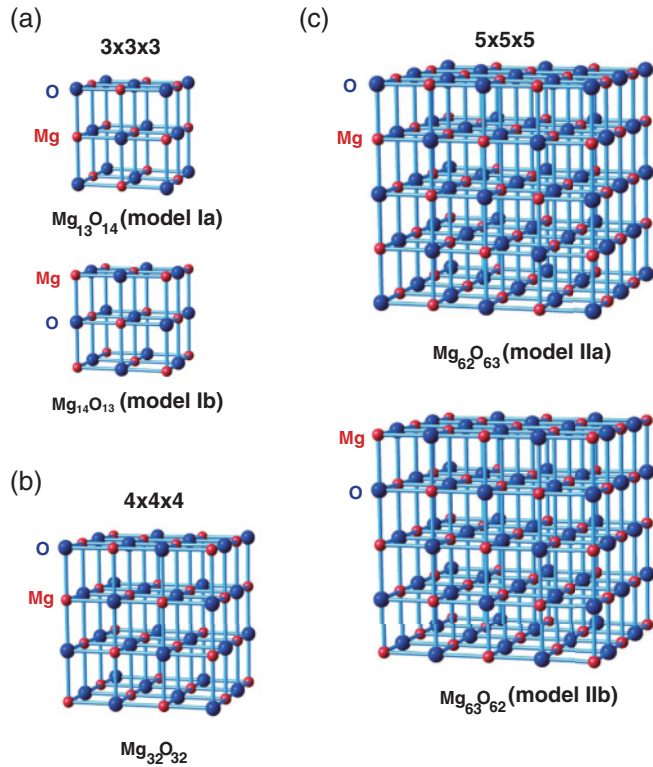


FIG. 1. (Color online) Cubic cluster models of MgO crystal. (a) A $(3 \times 3 \times 3)$ -atom block of nonstoichiometric composition: Mg₁₃O₁₄ (model Ia) and Mg₁₄O₁₃ (model Ib). (b) A $(4 \times 4 \times 4)$ -atom block of stoichiometric composition: Mg₃₂O₃₂. (c) A $(5 \times 5 \times 5)$ -atom block of nonstoichiometric composition: Mg₆₂O₆₃ (model IIa) and Mg₆₃O₆₂ (model IIb).

correlation functional of Lee, Yang, and Parr (B3LYP)¹⁷ with the GAUSSIAN-09 code.¹⁸ It has previously been shown that such a hybrid DFT functional is useful to correct the self-interaction problem,¹⁹ which often leads to misleading conclusions with regards to hole localization and the resulting magnetic characteristics of the system.^{11,20} We employed a series of cubic clusters with three different sizes (see Fig. 1),

a stoichiometric cluster with a $(4 \times 4 \times 4)$ -atom block and nonstoichiometric clusters with $(3 \times 3 \times 3)$ - and $(5 \times 5 \times 5)$ -atom blocks. As for the $3 \times 3 \times 3$ and $5 \times 5 \times 5$ clusters, we employed the following nonstoichiometric clusters: the Mg₁₃O₁₄ (model Ia) and Mg₆₂O₆₃ (model IIa) clusters, in which the eight corner atoms are O; and the Mg₁₄O₁₃ (model Ib) and Mg₆₃O₆₂ (model IIb) clusters, in which the eight corner atoms are Mg. Thus, models Ia and IIa (models Ib and IIb) correspond to Mg-deficient (O-deficient) composition. Starting from an ideal cubic configuration with an equal Mg-O interatomic distance of 2.1056 Å, which is the experimental Mg-O distance of the bulk MgO crystal, we fully optimized the geometry of the respective clusters for both spin-singlet ($S = 0$) and triplet ($S = 1$) states at the spin-restricted and spin-unrestricted B3LYP/6-31G(d) levels, respectively, without imposing any structural constraints. We found that the assumed cubic symmetry is almost retained for all model clusters after full geometry optimization irrespective of the spin state. We also found that the average Mg-O distance becomes shorter with decreasing the cluster size (see Table I), which is a general tendency of NaCl-type cubic clusters because of a lack of long-range repulsive interaction.²¹ The stability of the resulting optimized clusters was evaluated in terms of the atomization energy (AE), which is defined as the energy necessary to dissociate the Mg_mO_n cluster into neutral atoms ($m\text{Mg} + n\text{O}$), namely, $\text{AE} = mE(\text{Mg}) + nE(\text{O}) - E(\text{Mg}_m\text{O}_n)$,²² where $E(X)$ represents the total energy of the system X . The AE is useful to evaluate the stability of the clusters with the same dimension but different compositions and spin states.

As for the stoichiometric $4 \times 4 \times 4$ cluster, the nonmagnetic $S = 0$ ground state was correctly predicted, in agreement with the general consensus that MgO is a diamagnetic oxide. The energy separation between the singlet ($S = 0$) and triplet ($S = 1$) states, which is defined as $\Delta E_{t-s} = E(\text{triplet}) - E(\text{singlet})$, is 3.497 eV (see Table I), which is certainly too large to anticipate any magnetism from the stoichiometric cluster.

However, this is not necessarily the case for the nonstoichiometric clusters. The magnetic ($S = 1$) state was predicted

TABLE I. Structural and electronic properties of the cluster optimized at the B3LYP/6-31G(d) level in the respective spin states.

Composition of cluster	Spin state	Average Mg-O distance (Å)	E (a.u.) ^a	ΔE_{t-s} (eV) ^b	AE (eV) ^c
$(3 \times 3 \times 3)$					
Mg ₁₃ O ₁₄ (model Ia)	Singlet	2.026	-3655.83540		107.622
	Triplet	2.027	-3655.85187	-0.448	108.070
Mg ₁₄ O ₁₃ (model Ib)	Singlet	2.033	-3780.84324		107.326
	Triplet	2.031	-3780.82883	0.392	106.934
$(4 \times 4 \times 4)$ Mg ₃₂ O ₃₂	Singlet	2.052	-8814.72180		278.711
	Triplet	2.053	-8814.59331	3.497	275.215
$(5 \times 5 \times 5)$					
Mg ₆₂ O ₆₃ (model IIa)	Singlet	2.066	-17154.21466		557.162
	Triplet	2.063	-17154.23211	-0.475	557.634
Mg ₆₃ O ₆₂ (model IIb)	Singlet	2.068	-17279.21542		556.672
	Triplet	2.067	-17279.19929	0.439	556.233

^aThe total energy of the respective clusters in atomic unit (1 a.u. = 27.211383 eV).

^bThe energy separation between the singlet and triplet states.

^cThe atomization energy (AE) is defined as the energy necessary to dissociate the neutral (Mg_mO_n) cluster into neutral atoms ($m\text{Mg} + n\text{O}$).

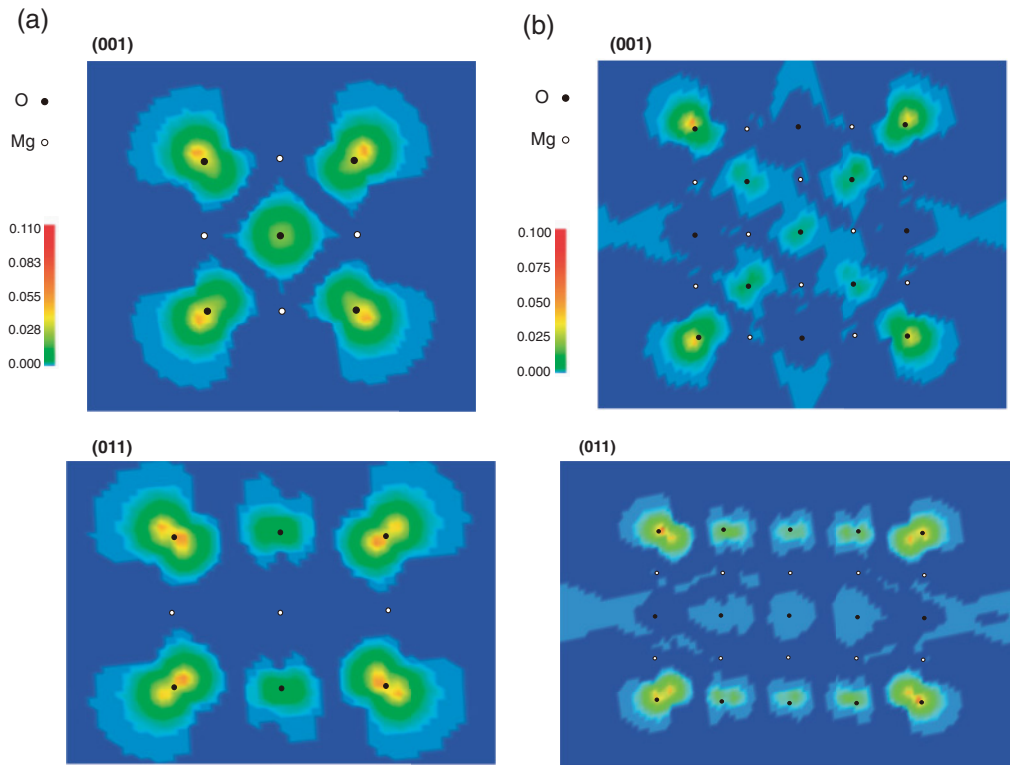


FIG. 2. (Color online) Spin density maps of (a) model Ia and (b) model IIa in the $S = 1$ state. Geometry optimization was performed at the B3LYP/6-31G(d) level. Upper and lower panels correspond to the results on the (001) and (011) planes, respectively.

to be more stable than the nonmagnetic ($S = 0$) state for Mg-deficient clusters, namely, models Ia and IIa, where the values of ΔE_{t-s} are -0.448 and -0.475 eV, respectively. On the other hand, the positive values of ΔE_{t-s} were predicted for O-deficient clusters (models Ib and IIb), implying that their ground state is the $S = 0$ state. It should be noted, however, that the atomization energies of the Mg-deficient clusters (models Ia and IIa) in the $S = 1$ state are larger than those of the corresponding O-deficient clusters (models Ib and IIb) in the $S = 0$ state. This allows us to predict that Mg-deficient clusters in the magnetic $S = 1$ state correspond to the most energetically stable spin state as far as the $3 \times 3 \times 3$ and $5 \times 5 \times 5$ clusters are concerned.

We next analyze the total spin density distribution, which is defined as the local density difference between the spin-up and spin-down states, in the magnetic $S = 1$ state of models Ia and IIa (see Fig. 2). Most of the spin density resides on the corner and surface O atoms. This indicates that the two holes derived from the deficiency in one Mg atom are preferentially located at $2p$ orbitals of the undercoordinated corner and surface oxygen atoms, showing a symmetrical and extended nature of the spin density distribution. This situation is quite different from that of O- $2p$ holes in a conventional cation vacancy in oxides, where the two holes are localized on two adjacent oxygen sites around the cation vacancy via polaronic distortion.²³

The spin polarization feature of these magnetic clusters can also be seen in the molecular orbital energy diagrams shown in Fig. 3. We see from Fig. 3 that the energy of the spin-down lowest unoccupied molecular orbital (LUMO) level, which is a doubly degenerate O- $2p$ state, is much lower than that of

the spin-up LUMO level. The obtained electronic structures hence show typical spin polarization characteristics achieved by hole doping at the spin-down LUMO level,²⁴ although the

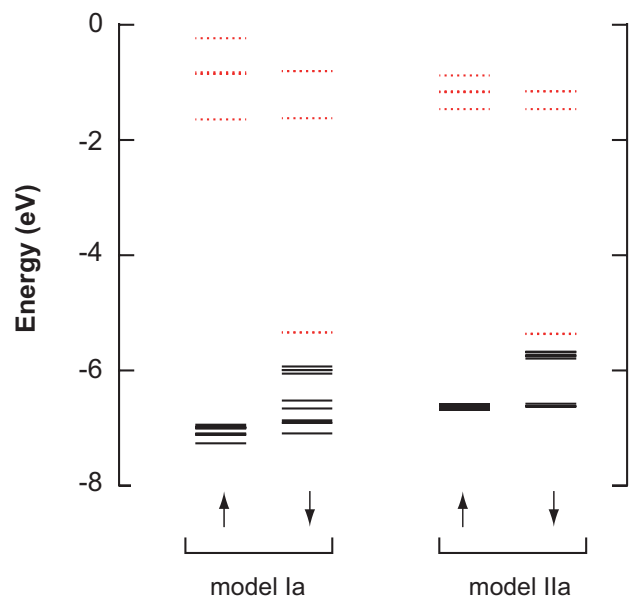


FIG. 3. (Color online) Molecular orbital energy-level diagram of the 10 highest occupied molecular orbitals (black solid lines) and the five lowest unoccupied molecular orbitals (red dotted lines) obtained for model Ia and model IIa in the $S = 1$ state.

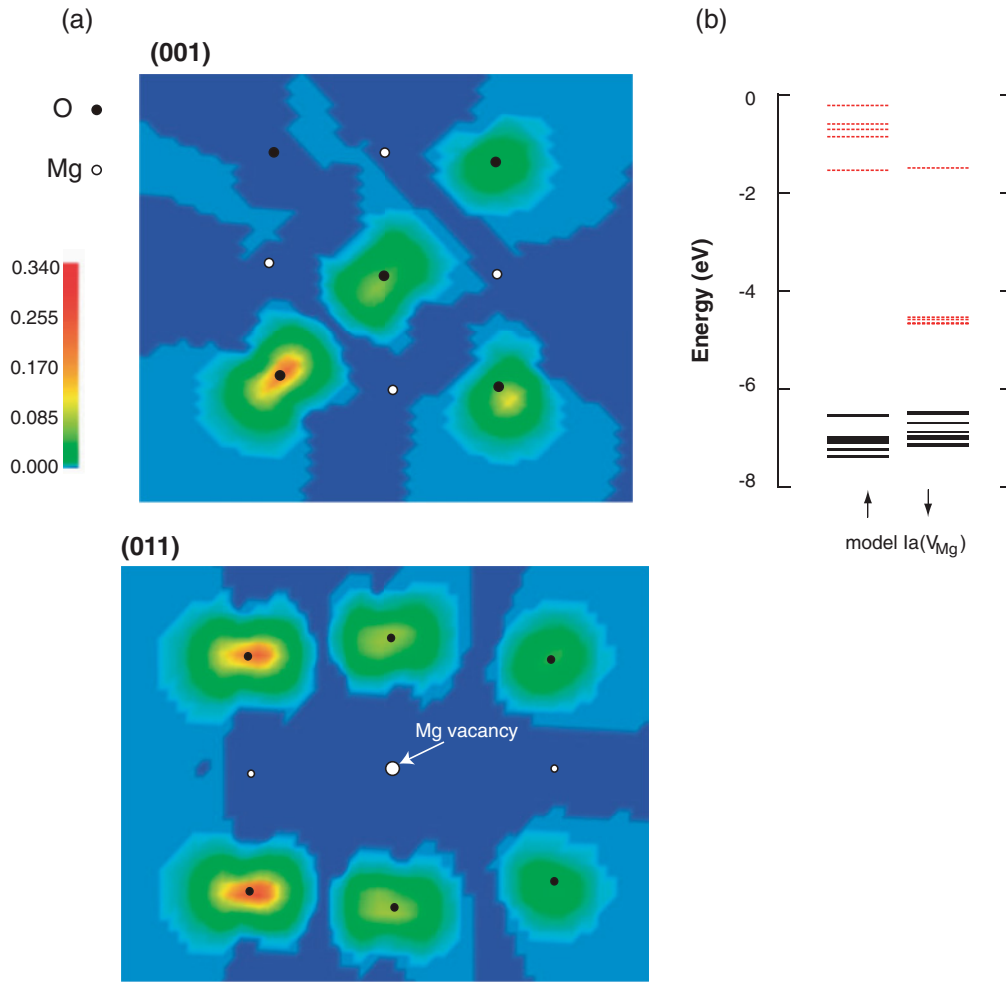


FIG. 4. (Color online) Electronic properties of the $\text{Mg}_{12}\text{O}_{14}$ cluster [model Ia(V_{Mg})] with one conventional Mg vacancy. Geometry optimization was performed at the B3LYP/6-31G(d) level in the quintuplet ($S = 2$) state. (a) Spin density maps on typical (001)- and (011)-like planes. (b) Molecular orbital energy-level diagram of the 10 highest occupied molecular orbitals (black solid lines) and the five lowest unoccupied molecular orbitals (red dotted lines).

LUMO is quite delocalized over the entire crystal structure in the present case.

It is also interesting to investigate the possible change in the spin state of the originally Mg-deficient cluster (model Ia or model IIa) with the introduction of further Mg vacancies. For that purpose, we intentionally removed one Mg atom located in the center of model Ia and performed geometry optimization of the resulting $\text{Mg}_{12}\text{O}_{14}$ cluster,²⁵ which is referred to as model Ia(V_{Mg}). We found that the optimization of model Ia(V_{Mg}) in the $S = 0$ and 1 states was not properly terminated because of the large displacement of the constituent atoms from the initial cubic-like configuration along with the problems in the self-consistent field convergence. We should note, however, that the optimized geometry in the quintuplet ($S = 2$) state was successfully obtained at the B3LYP/6-31G(d) level. Although the six oxygen atoms surrounding the Mg vacancy atoms were displaced outward with respect to the (001) surface, the optimized configuration in the $S = 2$ state still retains the cubic-like configuration. The above result suggests that the only realistic spin state of model Ia(V_{Mg}) is the quintuplet ($S = 2$) state with four unpaired electrons of parallel

spin. The resulting total spin density distribution and molecular orbital diagram are shown in Fig. 4. The spin density resides not only on the oxygen atoms adjacent to the central Mg vacancy but also on some of the corner oxygen atoms, similar to the case of model Ia in the $S = 1$ state. This indicates that the introduction of the Mg vacancy enables the higher spin state without deteriorating the extended nature of the spin density distribution of the original magnetic state, probably giving a reasonable account for the defect-enhanced ferromagnetism¹⁰ in nanoscale oxides.

Thus, the model of ferromagnetic order predicted in the cubic nonstoichiometric clusters is fundamentally different from the conventional one based on the m - J paradigm. The present model does not assume any long-range connectivity of local magnetic moments due to specific dopants and/or defects; rather, it predicts that the extended magnetic states are inherent characteristics of nanocrystals with a high structural symmetry and a stoichiometric deficiency. That is, the extended nature of spin distribution is inherently built into the symmetry and the destined compositional deficiency of nanocrystals. In that sense, long-range ferromagnetic order

is expected to be found in a variety of nanoscale oxides irrespective of the chemical composition, in harmony with the reported ubiquitous feature of ferromagnetism. Also, the present model allows us to assume that the direction of magnetic moment is determined by the symmetry and/or shape of each crystallite. Thus, the anisotropy of the magnetization observed often in polycrystalline thin films⁴ can be interpreted in terms of crystallographic anisotropy and/or the presence of a preferential growth direction in each crystallite. The present model may also give a reasonable account why dilute magnetic oxides exhibit ferromagnetism at doping concentrations well

below the percolation threshold.^{2,26} Since doping will promote nonstoichiometry of the oxide matrix, magnetization inherent to the nanocrystals will be enhanced by doping of atoms, either magnetic or nonmagnetic. We hence believe that the proposed model will shed new light on the origin of ferromagnetism not only in nondoped closed shell oxides but also in dilute magnetic semiconductors.

We thank the Supercomputer System, Institute for Chemical Research, Kyoto University, for providing the computer time to use the SGI Altix 4700 supercomputer.

*Corresponding author: Dr. Takashi Uchino, Department of Chemistry, Graduate School of Science, Kobe University, Nada, Kobe 657-8501, Japan; uchino@kobe-u.ac.jp

¹H. Ohno, H. Munekata, T. Penney, S. von Molnar, and L. L. Chang, *Phys. Rev. Lett.* **68**, 2664 (1992).

²J. M. D. Coey and S. A. Chambers, *MRS Bull.* **33**, 1953 (2008).

³H. Ohno, A. Shen, F. Matsukura, A. Oiwa, A. Endo, S. Katsumoto, and Y. Iye, *Appl. Phys. Lett.* **69**, 363 (1996).

⁴M. Venkatesan, C. B. Fitzgerald, and J. M. D. Coey, *Nature* **430**, 630 (2004).

⁵N. H. Hong, J. Sakai, N. Poiriot, and V. Brize, *Phys. Rev. B* **73**, 132404 (2006).

⁶A. Sundaresan, R. Bhargavi, N. Rangarajan, U. Siddesh, and C. N. R. Rao, *Phys. Rev. B* **74**, 161306(R) (2006).

⁷M. Stoneham, *J. Phys. Condens. Matter* **22**, 074211 (2010).

⁸J. Hu, Z. Zhang, M. Zhao, H. Qin, and M. Jiang, *Appl. Phys. Lett.* **93**, 192503 (2008).

⁹J. M. D. Coey, *Curr. Opin. Solid State. Mater. Sci.* **10**, 83 (2006).

¹⁰S. A. Chambers, *Surf. Sci. Rep.* **61**, 345 (2006).

¹¹A. Zunger, S. Lany, and H. Raebiger, *Physics* **3**, 53 (2010).

¹²A. M. Ferrari and G. Pacchioni, *J. Phys. Chem.* **99**, 17010 (1995).

¹³P. V. Sushko, A. L. Shluger, and C. R. A. Catlow, *Surf. Sci.* **450**, 153 (2000).

¹⁴D. Ricci, G. Pacchioni, P. V. Sushko, and A. L. Shluger, *J. Chem. Phys.* **117**, 2844 (2002).

¹⁵S. T. Bromley, I. de P. R. Moreira, K. M. Neyman, and F. Illas, *Chem. Soc. Rev.* **38**, 2657 (2009).

¹⁶A. D. Becke, *J. Chem. Phys.* **98**, 5648 (1993).

¹⁷C. Lee, W. Yang, and R. G. Parr, *Phys. Rev. B* **37**, 785 (1988).

¹⁸M. J. Frisch, G. W. Trucks, H. B. Schlegel, G. E. Scuseria, M. A. Robb, J. R. Cheeseman, G. Scalmani, V. Barone, B. Mennucci, G. A. Petersson, H. Nakatsuji, M. Caricato,

X. Li, H. P. Hratchian, A. F. Izmaylov, J. Bloino, G. Zheng, J. L. Sonnenberg, M. Hada, M. Ehara, K. Toyota, R. Fukuda, J. Hasegawa, M. Ishida, T. Nakajima, Y. Honda, O. Kitao, H. Nakai, T. Vreven, J. A. Montgomery Jr., J. E. Peralta, F. Ogliaro, M. Bearpark, J. J. Heyd, E. Brothers, K. N. Kudin, V. N. Staroverov, T. Keith, R. Kobayashi, J. Normand, K. Raghavachari, A. Rendell, J. C. Burant, S. S. Iyengar, J. Tomasi, M. Cossi, N. Rega, J. M. Millam, M. Klene, J. E. Knox, J. B. Cross, V. Bakken, C. Adamo, J. Jaramillo, R. Gomperts, R. E. Stratmann, O. Yazyev, A. J. Austin, R. Cammi, C. Pomelli, J. W. Ochterski, R. L. Martin, K. Morokuma, V. G. Zakrzewski, G. A. Voth, P. Salvador, J. J. Dannenberg, S. Dapprich, A. D. Daniels, O. Farkas, J. B. Foresman, J. V. Ortiz, J. Cioslowski, and D. J. Fox, GAUSSIAN 09 program, Revision B.01, Gaussian, Inc., Wallingford CT, 2010.

¹⁹M. Pesci, F. Gallino, C. Di Valentin, and G. Pacchioni, *J. Phys. Chem. C* **114**, 1350 (2010).

²⁰G. Pacchioni, F. Frigoli, D. Ricci, and J. A. Weil, *Phys. Rev. B* **63**, 054102 (2000).

²¹M. Riedler, A. R. B. de Castro, A. Kolmakov, J. O. Löfken, C. Nowak, A. V. Soldatov, A. Wark, A. Yalovega, and T. Möller, *Phys. Rev. B* **64**, 245419 (2001).

²²J. M. Recio and R. Pandey, *Phys. Rev. A* **47**, 2075 (1993).

²³A. Droghetti, C. D. Pemmaraju, and S. Sanvito, *Phys. Rev. B* **81**, 092403 (2010).

²⁴P. Mavropoulos, M. Ležaić, and S. Blügel, *Phys. Rev. B* **80**, 184403 (2009).

²⁵We also tried to perform DFT calculations by removing one Mg atom from model IIa. However, DFT calculations of the formed Mg₆₁O₆₃ cluster were quite time consuming because of the very slow convergence of SCF cycles and were not practically feasible in this Brief Report.

²⁶J. M. D. Coey, M. Venkatesan, and C. B. Fitzgerald, *Nat. Mater.* **4**, 173 (2005).